Extending the canopy flow model for natural, highly flexible macrophyte canopies

T.I. Marjoribanks & R.J. Hardy
Durham University, Durham, UK

S.N. Lane
UNIL Lausanne, Switzerland

D.R. Parsons
University of Hull, Hull, UK

ABSTRACT: Flow structures above vegetation canopies have received much attention within terrestrial and aquatic literature. This research has led to a good process understanding of mean and turbulent canopy flow structure. However, much of this research has focused on rigid or semi-rigid vegetation with relatively simple morphology. Aquatic macrophytes differ from this form, exhibiting more complex morphologies, predominantly horizontal posture in the flow and a different force balance. While some recent studies have investigated such canopies, there is still the need to examine the relevance and applicability of general canopy layer theory to these types of vegetation. Here, we report on a range of numerical experiments, using both semi-rigid and highly flexible canopies. The results for the semi-rigid canopies support existing canopy layer theory. However, for the highly flexible vegetation, the flow pattern is much more complex and suggests that a new canopy model may be required.

1 INTRODUCTION

Vegetation is a common feature within riverine environments and has a profound impact on channel and floodplain hydraulics. Vegetation increases channel resistance (Kouwen and Unny, 1973) which lowers the mean velocity (Jarvela, 2002, Nepf *et al.*, 2007) and, for a given discharge within a confined channel, leads to an increase in water depth. Hence, in-channel vegetation can pose a significant flood risk.

Conversely, there are many beneficial effects of in-channel vegetation. Vegetation canopies provide areas of decreased shear stress (Sukhodolov and Sukhodolova, 2010) which can create sediment and nutrient sinks that enable development of habitats for terrestrial and aquatic wildlife (Lopez and Garcia, 2001, Liu and Shen, 2008, Liu *et al.*, 2008). Vegetation also enhances ecosystem services, improving water quality through the production of oxygen and removal of heavy metals and nutrients (Kadlec and Knight, 1996).

Recognition of these issues has led to significant research on vegetated flows over the last two decades (Luhar and Nepf, 2013). This research, which has its origins in the terrestrial environment, has led to a good process understanding of turbulence structure above simple, idealized canopies such as crops (e.g. wheat) and grasses as commonly found in the terrestrial environment. Subsequent research within aquatic environments has built heavily upon this research, often applying similar assumptions regarding plant form.

However, aquatic macrophytes exhibit a much wider range of plant form and are often more complex in structure. Furthermore they are situated within a different fluid environment and are thus subject to different forces, namely buoyancy. Therefore, in order to apply the standard canopy flow model to the aquatic environment, it is first necessary to test it for these flows.

Here, we present results from numerical experiments designed to investigate flow structure over aquatic vegetation canopies. Two different combined biomechanical-flow models are applied, which between them provide information regarding a wide range of plant forms.

2 PREVIOUS RESEARCH INTO CANOPY FLOW STRUCTURE

One of the most significant challenges in understanding the impact of vegetation on flow has been characterizing the effect of vegetation on the mean velocity profile. Within un-vegetated open channel flows the velocity profile is assumed to follow the characteristic logarithmic profile associated with turbulent boundary layers. Vegetation has consequently been considered as a form of roughness within the channel and therefore treated as boundary

roughness term. This is accounted for using either roughness heights or roughness coefficients which adjust the predicted velocity accordingly.

However, vegetation is actually a porous mass blockage which can extend throughout the flow depth (Green, 2005). Therefore a boundary roughness assumption is no longer valid. Instead, the velocity profile resembles that of a mixing layer or free shear layer caused by two co-flowing streams of different velocity (Raupach *et al.*, 1996). This velocity difference between the two regions is induced by the drag discontinuity between the canopy flow and the flow above.

Inoue (1963) was the first to characterize this 'S' shaped velocity profile for terrestrial canopy flows. It has subsequently been refined into a 3 zone conceptual model of general canopy flow (Figure 1). The lower, emergent zone is characterized by pressure-driven flow and little, if any, vertical gradient in downstream velocity (Nepf and Vivoni, 2000). The middle layer, the mixing zone is characterized by an inflection point in the velocity profile that subsequently characterizes the canopy turbulence structure. The top layer, the log-law zone describes the region above the canopy top, where the flow profile is logarithmic (Lopez and Garcia, 2001). Within depth-limited shallow rivers, this zone is unlikely to fully develop (see Section 3.1).

Despite the importance of the emergent zone in defining the velocity profile, the zone of most interest with respect to canopy turbulence structure is the mixing zone as the mixing layer vortices account for up to 80% of the momentum transport between the canopy and the open flow (Ghisalberti and Nepf, 2009). In the mixing layer, the highly unstable inflection point in the velocity profile causes the development of Kelvin-Helmholtz (K-H) instabilities (Ikeda and Kanazawa, 1996). These are generated close to the canopy top and evolve downstream into spanwise roller vortices, which expand with distance and time (Ghisalberti and Nepf, 2002) before reaching a finite thickness when turbulent energy production equals dissipation (Ghisalberti and Nepf, 2004, 2006).

Finnigan *et al.* (2009) hypothesized that these roller vortices evolve further into a series of pairs of head-up and head-down hairpin vortices. Their terrestrial canopy data supported this hypothesis; however there has been limited high quality validation data to further test this idea over a wider range of terrestrial and, more importantly, aquatic canopies.

This highlights one of the key issues regarding previous work into canopy flow structure: the majority of research has been conducted either within the terrestrial environment (e.g. Raupach *et al.*, 1996, Py *et al.*, 2004, Finnigan *et al.*, 2009), or using highly simplified surrogate aquatic vegetation.

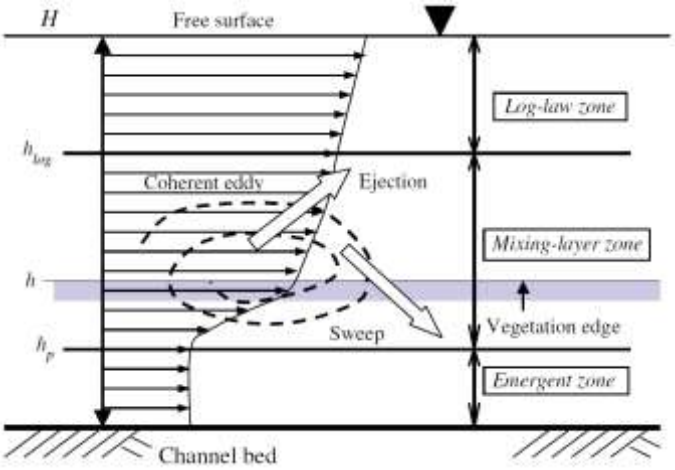

Figure 1. Schematic canopy flow model (reproduced from Nezu and Sanjou (2008) with permission from Elsevier).

For example, Ikeda and Kanawanza (1996) used nylon filaments to represent vegetation in their study, which was one of the first to find quantitative evidence of an inflected velocity profile within aquatic canopies. Okamoto and Nezu (2009) used a similar prototype vegetation in their Particle Image Velocimetry (PIV) experiments, detailing coherent structures over vegetation canopies.

Some studies have sought to investigate flow over more realistic aquatic canopies. For example, Wilson *et al.*, (2003) introduced artificial foliage onto stems within a flume study in order to study its effect on flow structure and found it had a noticeable effect. More recently, Siniscalchi *et al.*(2012) used a similar artificial canopy to investigate canopy flow structure. Their findings suggest the presence of large three-dimensional coherent structures above the canopy, though they only suggest that this might be controlled by K-H instabilities and they highlight the need for further investigation.

Finally, a few studies have used real vegetation, either within the field or flume environment. Sukhodolov and Sukhodolova (2010, 2012) have carried out experiments in natural rivers using *Sagittaria sagittifolia*. They found evidence of a mixing layer above a dense canopy, and developed a theoretical framework for predicting the vegetated mixing layer characteristics (Sukhodolova and Sukhodolov, 2012). These results suggest that canopy layer theory may be transferable to the aquatic case, but there is still the need to fully characterize flow dynamics within aquatic canopy flows.

3 DIFFERENCES BETWEEN TERRESTRIAL AND AQUATIC CANOPY FLOWS

As discussed above, much of the existing research has been conducted using canopies analogous to those found within terrestrial environments. Here we argue that there are three main differences between terrestrial and aquatic canopies which may lead to differences in canopy flow structure.

3.1 *Depth-limitation*

The first key difference is the depth-limited nature of aquatic canopy flows. The major impact of this is to alter the turbulent spectrum, increasing the dominance of K-H vortices within the turbulence regime (Nepf and Ghisalberti, 2008). A subsequent impact is that in cases with very low submergence depth, there may be inadequate depth for full development of the mixing layer. This may result in either a skewed or asymmetrical mixing layer.

3.2 *Biomechanics and force balance*

Aquatic vegetation exists within a very different environment to terrestrial vegetation. One of the key differences is the fluid density. Within the terrestrial environment, vegetation is universally denser than the fluid it resides in. Consequently, in a competitive environment, terrestrial plants often rely upon their flexural rigidity to counteract gravitational forces and reach sunlight. Within aquatic environments, the density difference is greatly reduced. Furthermore, many aquatic species have a lower density than the surrounding fluid and thus are positively buoyant (Luhar and Nepf, 2011) and therefore do not rely upon rigidity to compete for sunlight.

Rigidity can still be important and there are examples of aquatic plants with high rigidity (e.g. reeds), however, these often tend to be emergent plants. The majority of macrophytes exhibit low rigidity. One reason for this is that aquatic plants can experience a drag force 25 times larger than terrestrial plants for a given velocity (Denny and Gaylord, 2002). Therefore, low rigidity enables aquatic plants to reconfigure within the flow to minimize the drag and prevent uprooting or damage (Sand-Jensen, 2003). Thus, the ratio between the different internal (buoyancy, rigidity) and external (drag) forces is significantly different between terrestrial and aquatic canopy flows.

3.3 *Posture and form*

As a result of the different force balance, aquatic canopies exhibit a distinct posture within the flow. Due to plant reconfiguration, many aquatic plants adopt a horizontal position within the flow, which is a departure from the idealized, perpendicular canopy structure used within terrestrial canopies and many aquatic prototype experiments (e.g. Nepf, 1999, Dunn *et al.*, 1996). It is therefore likely that plant-flow interactions will reflect that.

Aquatic vegetation must find a balance between drag reduction and photosynthetic capacity (Albayrak *et al.*, 2011, Bal *et al.*, 2011). Therefore, aquatic vegetation commonly has substantial foliage with a large surface area to maximize light capture. As a result, aquatic vegetation is often characterized by complex plant forms, which the general canopy layer model does not account for. This may be significant in terms of flow structure as foliage can inhibit momentum exchange between the canopy flow and the flow above (Wilson *et al.*, 2003).

4 METHODOLOGY

In order to investigate canopy flow structure over aquatic canopies, two biomechanical models were employed within a high resolution computational fluid dynamics (CFD) framework. The advantage of modelling over flume or field work is that it enables investigation of the entire flow-field, within and above the canopy, under controlled hydraulic and biomechanical conditions. Details of both models can be found in Marjoribanks *et al.*, (in review) and only a synopsis is provided here.

The two models were conceptualized within Nikora's (2010) framework which distinguishes between semi-rigid bending force dominated vegetation and highly flexible vegetation where tensile forces dominate. This provides a useful framework for analyzing vegetation across a range of plant forms.

4.1 *Euler-Bernoulli Beam equation model*

For semi-rigid, bending vegetation which is controlled predominantly by the force balance between the flow and internal rigidity, an Euler-Bernoulli beam equation model is used. The Euler-Bernoulli beam equation is a partial differential equation which solves the deflection of a thin cantilever beam under external loading. It balances the external forces against the internal flexural rigidity force which is a function of stem morphology and biomechanics.

The cantilever approximation has been used previously as a basis for vegetation models. Firstly, in developing a canopy-scale physical model of vegetation within a terrestrial environment, Finnigan and Mulhearn (1978) approximated the stems as cantilevers, thus enabling the application of a version of the Euler-Bernoulli beam equation to characterize the flexural properties of the waving crops.

Kutija and Hong (1996) used a simplified cantilever beam approach to calculate the effective height of vegetation, and consequently the velocity profile for vegetated flows. Erduran and Kutija (2003) used a similar approach to develop a quasi-three-dimensional CFD model for flexible vegetation canopies.

Ikeda *et al.* (2001) used the Euler-Bernoulli beam equation to drive a biomechanical model within a two-dimensional large eddy simulation (LES) framework. In their study the vegetation stems were modelled explicitly in contrast to the earlier models which were canopy-scale.

The model used here is similar to Ikeda *et al.*'s model, using dual plant and LES grids to transfer information between the biomechanical model and the flow model.

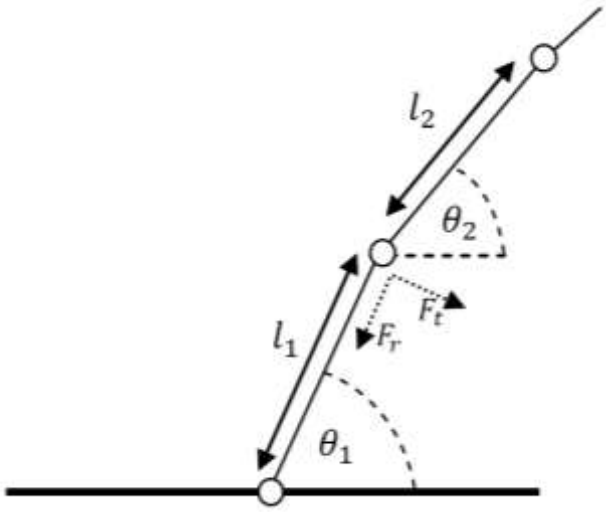

Figure 2: N-pendula schematic. Here, pendula of length l_i are connected by hinge joints (circles). The force at each node is resolved into transverse (F_t) and radial (F_r) components.

4.2 *N-pendula model*

For modelling highly flexible, tensile vegetation, an N-pendula model was used. The N-pendula model is conceptually very different to the Euler-Bernoulli beam model as it solves the plant dynamics locally rather than globally as is the case with a partial differential equation. Instead of using a global equation, the N-pendula model is conceptualized as a series of pendula connected by hinges or pivots (Figure 2).

Each pendulum is subject to a moment about its pivot which is calculated as the balance between the local external fluid forces and internal resistive forces. These forces are resolved into a transverse component (which becomes the local moment) and a radial component which is transferred to the force balance at the neighboring pendula (Figure 2).

Similar to the Euler-Bernoulli beam model, the N-pendula approach has also been used in previous studies to represent vegetation. Abdelrhman (2007) developed a model using this approach, however it was implemented within a simplified flow model based upon known velocity profile and was unable to fully represent the dynamic interaction between the flow and vegetation.

Dijkstra and Uittenbogaard (2010) extended this approach, introducing a rigidity treatment into the N-pendula model. However, the model proved to be highly sensitive to the rigidity parameter, which was difficult to measure with accuracy. In contrast with Abdelrhman (2007) they used a more complex Reynolds-Averaged Navier-Stoke (RANS) based flow model enabling them to resolve the flow field using CFD. However, the RANS method is still unable to predict fully the time-dependent turbulent characteristics and consequent vegetation response.

In this study, an N-pendula model with a simplified rigidity treatment is applied. This is justifiable as the model is designed to represent vegetation where rigidity is not the main driving force.

4.3 *Numerical experiments*

Both biomechanical models were implemented within a high-resolution CFD framework using a dynamic mass flux scaling algorithm, based upon previous work modelling flow over complex topography (Lane *et al.*, 2002). LES was used in order to fully resolve the large scale eddies of interest, without the computational restrictions of Direct Numerical Simulation (DNS). The grid resolution (0.002 m) was chosen such that the plant diameter (0.01 m) was at least four times the grid resolution as this ensured that wake-scale turbulence was resolved and was shown to improve numerical convergence dramatically (Marjoribanks, 2013).

In order to investigate canopy flows over a range of conditions, experiments were carried out using two different vegetation configurations within each model. These two configurations consisted of i) a single patch of vegetation and ii) a continuous vegetation canopy. These were designed to distinguish between the case of sparse canopies consisting of small patches of vegetation, and entire continuous canopies with high stem density throughout.

The flow conditions were chosen such that the flow was fully turbulent (Re = 12 000-23 000) and subcritical (Fr = 0.17-0.29). These conditions corresponded to inlet velocities of U = 0.3-0.7 ms^{-1}. Recirculating boundary conditions were applied in the downstream direction to allow simulation of long continuous canopies. At the bed, a no-slip condition was applied with a logarithmic law of the wall treatment, instead of varying the cell size in the near-wall region. At the lateral boundaries, a frictionless wall boundary was applied.

5 RESULTS

Two methods were applied in order to extract information regarding large scale coherent turbulent structures. Firstly, normalized velocity profiles were analyzed in order to identify the presence of a vegetated mixing layer. The mixing layer velocity profile dictates the generation of canopy-scale vortices and therefore the velocity profile is useful in determining the presence of large-scale turbulent structures. Secondly, vortex detection methods were applied to the data. These included Eulerian (Q criterion) and Lagrangian (FTLE) methods as well as vorticity (Hunt *et al.*, 1988, Haller, 2000).

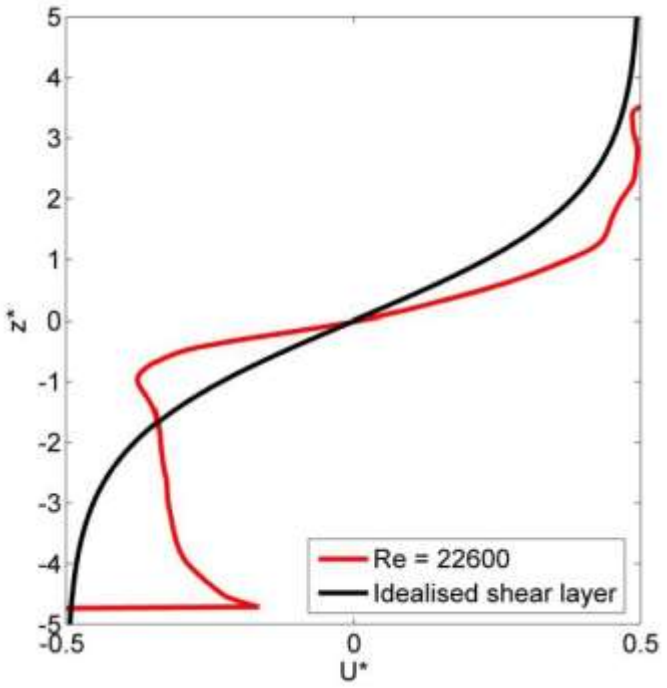

Figure 3. Normalized velocity profile for the horizontally and temporally averaged downstream velocity in the semi-rigid patch simulation. The idealized shear layer profile is in black. Normalized variables were calculated as $z^* = (z - \bar{z})/\theta_M$and $u^* = (U - \overline{U})/\Delta U$, where ΔU is the mixing layer velocity difference, $\theta_M$is the momentum thickness, and $\overline{U}$ is the mean mixing layer velocity, which occurs at the height $z = \bar{z}$.

5.1 *Semi-rigid patch*

For the semi-rigid patch simulation, the normalized velocity profile shows a clear inflection point which agrees well with that expected for an ideal mixing layer (Figure 3). The velocity profile shows increased velocity in the near-bed region, which is consistent with Stoesser *et al.* (2006) who suggested it originated from the necklace/horseshoe vortices that form around individual plant stems.

The vorticity and FLTE plots (Figure 4) show the presence of a Kelvin-Helmholtz vortex at the canopy top which is recirculated through the domain, and decreases in strength but increases in size through time. Both the vortex centers (shown by the vorticity plot) and vortex ridges (shown by the FTLE plot) are consistent throughout the time series. The FTLE does not pick up the entire vortex, with the upper limb appearing much stronger than the lower limb, however combined with the vorticity results; there is substantial evidence of vortices similar to those expected according to the canopy layer model.

5.2 *Semi-rigid canopy*

For the semi-rigid canopy simulation, the normalized velocity profile again shows good agreement with the idealized shear layer profile (Figure 5). In this case, the interface at the canopy top is particularly sharp, suggesting an asymmetrical shear layer.

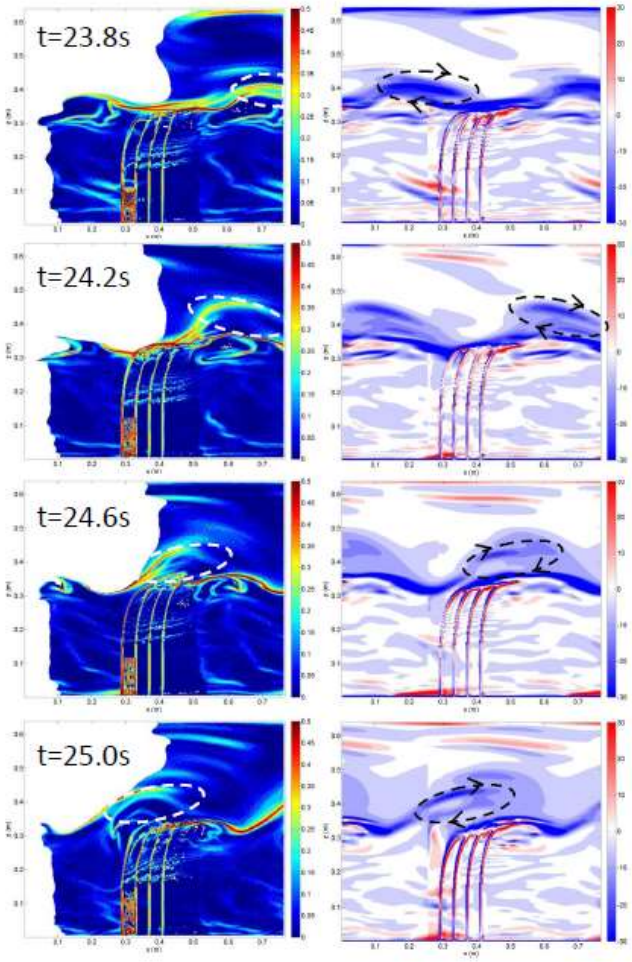

Figure 4. FTLE (left) and vorticity (right) long-sections at a series of time-steps. The positions of identified vortices are shown using the dotted ovals. The white regions in the FTLE plot correspond to regions where the trajectories could not be fully tracked. In the vorticity plots, blue corresponds to clockwise vorticity and red to anti-clockwise vorticity

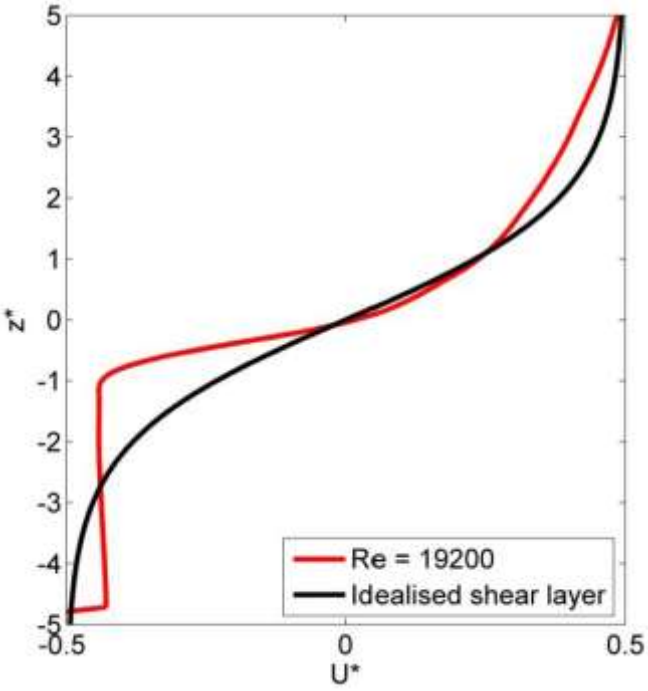

Figure 5. Normalised velocity profile for the horizontally and temporally averaged downstream velocity in the semi-rigid canopy simulation. The idealized shear layer profile is shown in black

The vortex detection methods both identify a large-scale canopy shear layer vortex moving along the top of the canopy (Figure 6). The vortex is more clearly defined in the FTLE image in this case, with a clear upper and lower limb of the roller vortex present. It is possible that this FTLE signature corresponds to a hairpin vortex (Green *et al.*, 2007) as hypothesized by Finnigan *et al.* (2009). However, further three-dimensional analysis would be required in order to confirm this.

The *Q* criterion results coincide well with the FTLE results, confirming the presence of a roller vortex at the canopy top. The vortex center is noticeably displaced above the canopy top. This is in agreement with Ghisalberti and Nepf (2002) who found that the height of the vortex center increases through time due to the effect of the canopy drag.

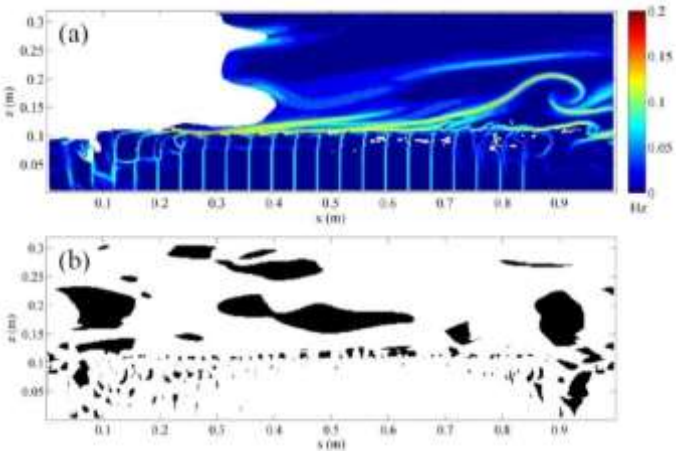

Figure 6. Vortex detection results using the (a) FTLE and (b) *Q* criterion. In (a), areas in yellow/red represent vortex ridges. In (b), areas of black represent vortices.

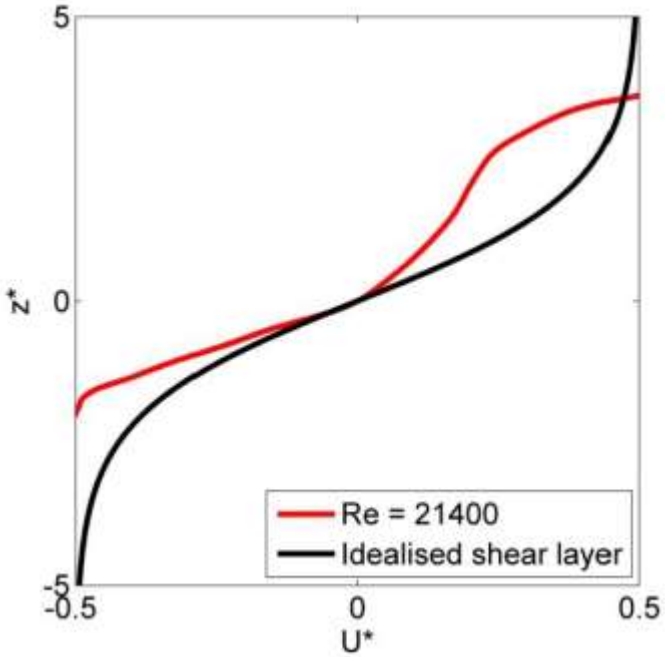

Figure 7. Normalised velocity profile for the horizontally and temporally averaged downstream velocity in the highly flexible patch simulation. The idealized shear layer profile is shown in black

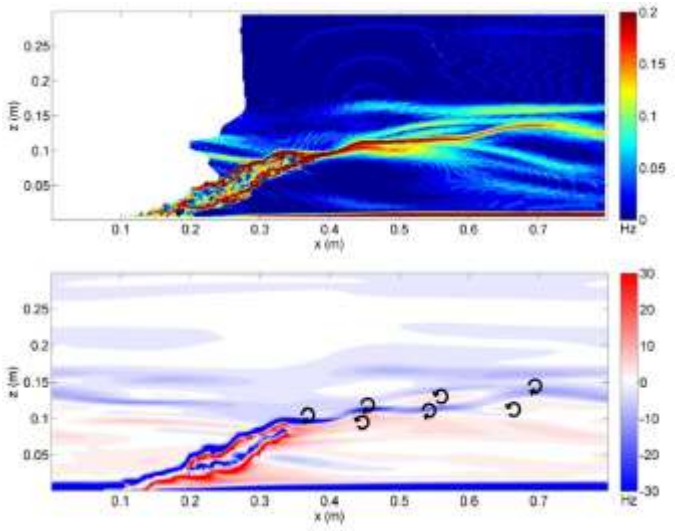

Figure 8. Vortex detection results using the (a) FTLE and (b) vorticity. In (a), areas in yellow/red represent vortex ridges. In (b), blue corresponds to clockwise vorticity and red to anti-clockwise vorticity.

5.3 *Highly flexible patch*

For the highly flexible patch simulation, the normalized velocity profile shows less agreement with the idealized mixing layer profile (Figure 7). Although there is some evidence of an inflection point in the velocity profile, it is much less well defined. This suggests that canopy-scale vortices may not dominate the flow regime in the same way as in the semi-rigid cases.

The FTLE plot (Figure 8) indicates the presence of vorticity at and around the top of the vegetation, however, it is unclear whether this corresponds to canopy shear layer vorticity. The corresponding vorticity plot suggests that although there is a general dominance of anti-clockwise vorticity along the canopy top, the majority of the turbulence highlighted in Figure 8 appears to correspond to plant-flapping induced vorticity (Nikora, 2010). Here, the vortex mechanism appears similar to that of wake-scale shedding, although the vortices are larger than those produced by stem wake-shedding.

5.4 *Highly flexible canopy*

For the highly flexible canopy, the normalized velocity profile shows very good geometric agreement with the idealized shear layer profile (Figure 9). This suggests that in contrast to the patch case, canopy layer turbulence may dominate.

The FTLE results (Figure 10) indicate a highly complex pattern of turbulence at the canopy top. Results from the other vortex detection methods are not included for this case as they were not helpful in characterizing the canopy turbulence.

There is some evidence of Kelvin-Helmholtz vortices appearing in the region at the canopy top, though this pattern appears to change significantly

through time. There also appears to be evidence of flapping-scale vortices, as with the patch case.

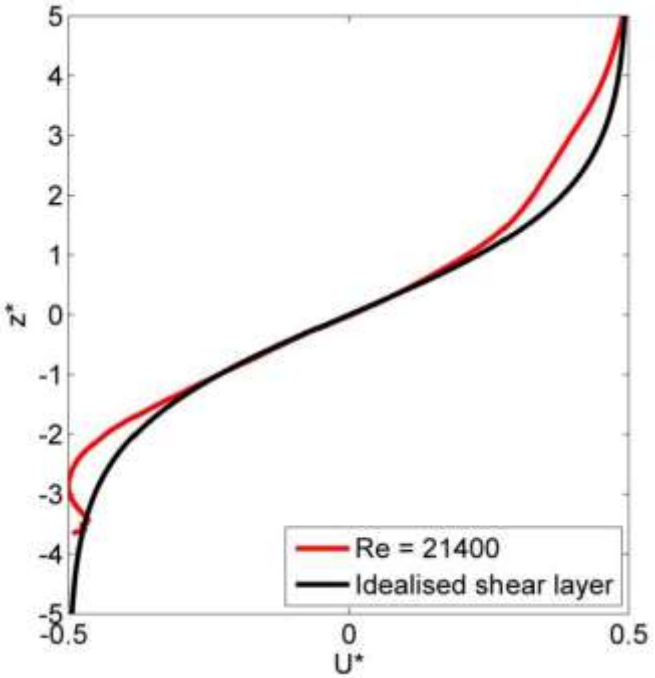

Figure 9. Normalised velocity profile for the horizontally and temporally averaged downstream velocity in the highly flexible canopy simulation. The idealized shear layer profile is shown in black

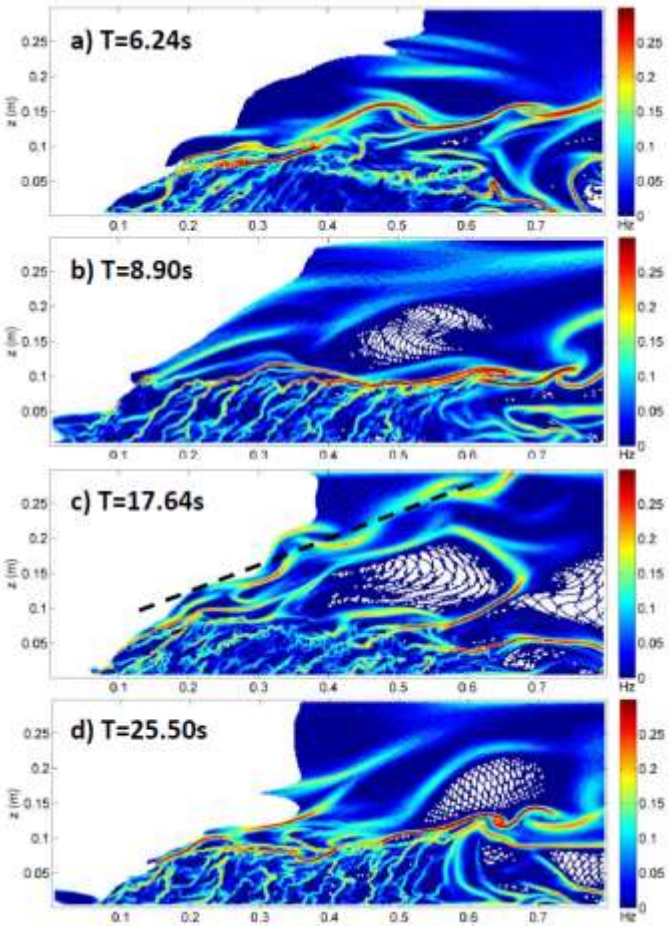

Figure 10. FTLE snapshots from the highly flexible canopy simulation. Areas in yellow/red represent vortex ridges

6 CONCLUSIONS

The results from the numerical model demonstrate that across the range of plant forms, vegetation has a significant impact on turbulence, though this effect varies dependent upon plant characteristics. Notably, for the semi-rigid canopies, the turbulent energy budget is dominated by canopy-scale roller vortices. In contrast, for highly flexible canopies, a third, plant-flapping scale turbulence scale emerges (Nikora, 2010). This scale appears similar to a vortex shedding mechanism from the tail of a flag (Michelin *et al.*, 2008) and represents a much larger contribution to the turbulent energy budget than the wake-scale vortex shedding.

In light of these results, we suggest that the current canopy layer model requires modification for complex aquatic macrophyte canopies. In such cases, whilst a vegetated mixing layer may still exist for high density canopies, 'plant-flapping' scale vortices play a significant role within the turbulent kinetic energy budget. Therefore we suggest that further research is required in order to develop a canopy model which is applicable across a range of forms.

REFERENCES

Abdelrhman, M. A. (2007) Modeling coupling between eelgrass Zostera marina and water flow. *Marine Ecology Progress Series,* 338**,** 81-96.

Albayrak, I., Nikora, V., Miler, O. & O'hare, M. (2011) Flow-plant interactions at a leaf scale: effects of leaf shape, serration, roughness and flexural rigidity. *Aquatic Sciences - Research Across Boundaries***,** 1-20.

Bal, K. D., Bouma, T. J., Buis, K., Struyf, E., Jonas, S., Backx, H. & Meire, P. (2011) Trade-off between drag reduction and light interception of macrophytes: comparing five aquatic plants with contrasting morphology. *Functional Ecology,* 25**,** 1197-1205.

Denny, M. & Gaylord, B. (2002) The mechanics of wave-swept algae. *Journal of Experimental Biology,* 205**,** 1355-1362.

Dijkstra, J. T. & Uittenbogaard, R. E. (2010) Modeling the interaction between flow and highly flexible aquatic vegetation. *Water Resour. Res.,* 46**,** W12547.

Dunn, C., Lopez, F. & Garcia, M. H. (1996) Mean flow and turbulence in a laboratory channel with simulated vegetation. *Hydrosystems laboratory hydraulic engineering series.* Urbana, University of Illinois.

Erduran, K. S. & Kutija, V. (2003) Quasi-three-dimensional numerical model for flow through flexible, rigid, submerged and non-submerged vegetation. *Journal of Hydroinformatics,* 5**,** 189-202.

Finnigan, J. J. & Mulhearn, P. J. (1978) Modelling waving crops in a wind tunnel. *Boundary-Layer Meteorology,* 14**,** 253-277.

Finnigan, J. J., Shaw, R. H. & Patton, E. G. (2009) Turbulence structure above a vegetation canopy. *Journal of Fluid Mechanics,* 637**,** 387-424.

Ghisalberti, M. & Nepf, H. M. (2002) Mixing layers and coherent structures in vegetated aquatic flows. *Journal of Geophysical Research-Oceans,* 107**,** 11.

Ghisalberti, M. & Nepf, H. M. (2004) The limited growth of vegetated shear layers. *Water Resour. Res.,* 40**,** W07502.

Ghisalberti, M. & Nepf, H. M. (2006) The Structure of the Shear Layer in Flows over Rigid and Flexible Canopies. *Environmental Fluid Mechanics,* 6**,** 277-301.

Ghisalberti, M. & Nepf, H. M. (2009) Shallow Flows Over a Permeable Medium: The Hydrodynamics of Submerged Aquatic Canopies. *Transport in Porous Media,* 78**,** 385-402.

Green, J. C. (2005) Modelling flow resistance in vegetated streams: review and development of new theory. *Hydrological Processes,* 19**,** 1245-1259.

Green, M. A., Rowley, C. W. & Haller, G. (2007) Detection of Lagrangian coherent structures in three-dimensional turbulence. *Journal of Fluid Mechanics,* 572**,** 111-120.

Haller, G. (2000) Finding finite-time invariant manifolds in two-dimensional velocity fields. *Chaos: An Interdisciplinary Journal of Nonlinear Science,* 10**,** 99-108.

Hunt, J. C. R., Wray, A. A. & Moin, P. (1988) Eddies, stream and convergence zones in turbulent flows. *Center for Turbulence Research Report.*

Ikeda, S. & Kanazawa, M. (1996) Three-dimensional organized vortices above flexible water plants. *Journal of Hydraulic Engineering-Asce,* 122**,** 634-640.

Ikeda, S., Yamada, T. & Toda, Y. (2001) Numerical study on turbulent flow and honami in and above flexible plant canopy. *International Journal of Heat and Fluid Flow,* 22**,** 252-258.

Inoue, E. (1963) On the Turbulent Structure of Airflow within Crop Canopies. *Journal of the Meteorological Society of Japan. Ser II,* 41**,** 317-326.

Jarvela, J. (2002) Flow resistance of flexible and stiff vegetation: a flume study with natural plants. *Journal of Hydrology,* 269**,** 44-54.

Kadlec, R. H. & Knight, R. L. (1996) *Treatment Wetlands,* Boca Raton, FL, Lewis Publishers.

Kouwen, N. & Unny, T. E. (1973) Flexible roughness in open channels. *Journal of the Hydraulics Division-Asce,* 101**,** 194-196.

Kutija, V. & Hong, H. T. M. (1996) A numerical model for assessing the additional resistance to flow introduced by flexible vegetation. *Journal of Hydraulic Research,* 34**,** 99-114.

Lane, S. N., Hardy, R. J., Elliott, L. & Ingham, D. B. (2002) High-resolution numerical modelling of three-dimensional flows over complex river bed topography. *Hydrological Processes,* 16**,** 2261-2272.

Liu, C. & Shen, Y.-M. (2008) Flow structure and sediment transport with impacts of aquatic vegetation. *Journal of Hydrodynamics, Ser. B,* 20**,** 461-468.

Liu, D., Diplas, P., Fairbanks, J. D. & Hodges, C. C. (2008) An experimental study of flow through rigid vegetation. *J. Geophys. Res.,* 113.

Lopez, F. & Garcia, M. H. (2001) Mean flow and turbulence structure of open-channel flow through non-emergent vegetation. *Journal of Hydraulic Engineering-Asce,* 127**,** 392-402.

Luhar, M. & Nepf, H. M. (2011) Flow-induced reconfiguration of buoyant and flexible aquatic vegetation. *Limnology and Oceanography,* 56**,** 2003-2017.

Luhar, M. & Nepf, H. M. (2013) From the blade scale to the reach scale: A characterization of aquatic vegetative drag. *Advances in Water Resources,* 51**,** 305-316.

Marjoribanks, T. (2013) *High resolution modelling of flexible submerged vegetation in rivers*. PhD**,** Durham University

Marjoribanks, T., Hardy, R. J., Lane, S. N. & Parsons, D. R. (in review) High resolution modelling of flow-vegetation interactions. *Journal of Hydraulic Research*.

Michelin, S., Smith, S. G. L. & Glover, B. J. (2008) Vortex shedding model of a flapping flag. *Journal of Fluid Mechanics,* 617**,** 1-10.

Nepf, H. & Ghisalberti, M. (2008) Flow and transport in channels with submerged vegetation. *Acta Geophysica,* 56**,** 753-777.

Nepf, H., Ghisalberti, M., White, B. & Murphy, E. (2007) Retention time and dispersion associated with submerged aquatic canopies. *Water Resources Research,* 43**,** 10.

Nepf, H. M. (1999) Drag, turbulence, and diffusion in flow through emergent vegetation. *Water Resources Research,* 35**,** 479-489.

Nepf, H. M. & Vivoni, E. R. (2000) Flow structure in depth-limited, vegetated flow. *Journal of Geophysical Research-Oceans,* 105**,** 28547-28557.

Nezu, I. & Sanjou, M. (2008) Turburence structure and coherent motion in vegetated canopy open-channel flows. *Journal of Hydro-environment Research,* 2**,** 62-90.

Nikora, V. (2010) Hydrodynamics of aquatic ecosystems: An interface between ecology, biomechanics and environmental fluid mechanics. *River Research and Applications,* 26**,** 367-384.

Okamoto, T.-A. & Nezu, I. (2009) Turbulence structure and "Monami" phenomena in flexible vegetated open-channel flows. *Journal of Hydraulic Research,* 47**,** 13.

Py, C., De Langre, E. & Moulia, B. (2004) The mixing layer instability of wind over a flexible crop canopy. *Comptes Rendus Mécanique,* 332**,** 613-618.

Raupach, M. R., Finnigan, J. J. & Brunet, Y. (1996) Coherent eddies and turbulence in vegetation canopies: The mixing-layer analogy. *Boundary-Layer Meteorology,* 78**,** 351-382.

Sand-Jensen, K. (2003) Drag and reconfiguration of freshwater macrophytes. *Freshwater Biology,* 48**,** 271-283.

Siniscalchi, F., Nikora, V. I. & Aberle, J. (2012) Plant patch hydrodynamics in streams: Mean flow, turbulence, and drag forces. *Water Resour. Res.,* 48**,** W01513.

Stoesser, T., Liang, C., Rodi, W. & Jirka, G. (2006) Large eddy simulation of fully-developed turbulent flow through submerged vegetation. *River Flow 2006, Two Volume Set.* Taylor & Francis.

Sukhodolov, A. N. & Sukhodolova, T. A. (2010) Case Study: Effect of Submerged Aquatic Plants on Turbulence Structure in a Lowland River. *Journal of Hydraulic Engineering,* 136**,** 434-446.

Sukhodolov, A. N. & Sukhodolova, T. A. (2012) Vegetated mixing layer around a finite-size patch of submerged plants: Part 2. Turbulence statistics and structures. *Water Resources Research,* 48**,** n/a-n/a.

Sukhodolova, T. A. & Sukhodolov, A. N. (2012) Vegetated mixing layer around a finite-size patch of submerged plants: 1. Theory and field experiments. *Water Resources Research,* 48**,** n/a-n/a.

Wilson, C., Stoesser, T., Bates, P. D. & Pinzen, A. B. (2003) Open channel flow through different forms of submerged flexible vegetation. *Journal of Hydraulic Engineering-Asce,* 129**,** 847-853.